

## Article

# Fungal Secondary Metabolites/Dicationic Pyridinium Iodide Combinations in Combat against Multi-Drug Resistant Microorganisms

Ayoub M. Abdelatif<sup>1</sup>, Bassma H. Elwakil<sup>2,\*</sup> , Mohamed Zakaria Mohamed<sup>3</sup> , Mohamed Hagar<sup>3</sup>  and Zakia A. Olama<sup>1</sup>

<sup>1</sup> Department of Botany & Microbiology, Faculty of Science, Alexandria University, Alexandria 21568, Egypt

<sup>2</sup> Department of Medical Laboratory Technology, Faculty of Applied Health Sciences Technology, Pharos University in Alexandria, Alexandria 21526, Egypt

<sup>3</sup> Department of Chemistry, Faculty of Science, Alexandria University, Alexandria 21568, Egypt

\* Correspondence: bassma.hassan@pua.edu.eg

**Abstract:** The spread of antibiotic-resistant opportunistic microbes is a huge socioeconomic burden and a growing concern for global public health. In the current study, two endophytic fungal strains were isolated from *Mangifera Indica* roots and identified as *Aspergillus niger* MT597434.1 and *Trichoderma lixii* KU324798.1. Secondary metabolites produced by *A. niger* and *T. lixii* were extracted and tested for their antimicrobial activity. The highest activity was noticed against *Staphylococcus aureus* and *E. coli* treated with *A. niger* and *T. lixii* secondary metabolites, respectively. *A. niger* crude extract was mainly composed of Pentadecanoic acid, 14-methyl-, methyl ester and 9-Octadecenoic acid (Z)-, methyl ester (26.66 and 18.01%, respectively), while *T. lixii* crude extract's major components were 2,4-Decadienal, (E,E) and 9-Octadecenoic acid (Z)-, and methyl ester (10.69 and 10.32%, respectively). Moreover, a comparative study between the fungal extracts and dicationic pyridinium iodide showed that the combination of *A. niger* and *T. lixii* secondary metabolites with dicationic pyridinium iodide compound showed a synergistic effect against *Klebsiella pneumoniae*. The combined formulae inhibited the bacterial growth after 4 to 6 h through cell wall breakage and cells deformation, with intracellular components leakage and increased ROS production.

**Keywords:** endophytic fungi; *Trichoderma lixii*; *Aspergillus niger*; dicationic pyridinium iodide; multi-drug resistant



**Citation:** Abdelatif, A.M.; Elwakil, B.H.; Mohamed, M.Z.; Hagar, M.; Olama, Z.A. Fungal Secondary Metabolites/Dicationic Pyridinium Iodide Combinations in Combat against Multi-Drug Resistant Microorganisms. *Molecules* **2023**, *28*, 2434. <https://doi.org/10.3390/molecules28062434>

Academic Editor: Faiza Diaba

Received: 31 January 2023

Revised: 2 March 2023

Accepted: 3 March 2023

Published: 7 March 2023



**Copyright:** © 2023 by the authors. Licensee MDPI, Basel, Switzerland. This article is an open access article distributed under the terms and conditions of the Creative Commons Attribution (CC BY) license (<https://creativecommons.org/licenses/by/4.0/>).

## 1. Introduction

The emergence of multidrug-resistant microorganisms has increased the urgency of finding effective new antimicrobials to treat bacterial, fungal, and viral illnesses in humans and animals [1].  $\beta$ -lactam resistance emergence in Gram-negative bacteria has been a major concern that has become an obstacle in the treatment of infectious diseases, especially those caused by *Klebsiella pneumoniae*. Miryala et al. [2] studied the role of the SHV-11 gene in drug resistance mechanism patterns in a *K. pneumoniae* strain. It was concluded that the SHV11 gene, along with the functional partners, were not only responsible for the drug resistance mechanism, but also helped in maintaining the genomic integrity through the DNA damage repair mechanism.

On the other hand, endophytic fungi are a broad collection of microorganisms that live either entirely or partially inside the cells of their host plants, invading healthy tissues with no outward sign of illness [3]. More and more chemicals with diverse biological functions are being extracted from endophytic fungi [4]. Natural products with biological functions which are called secondary metabolites and endophytic filamentous fungi are among the most prolific producers [4]. Many useful bioactive chemicals with antibacterial, insecticidal, cytotoxic, and anticancer activities have been isolated in the last two decades from

endophytic fungi [5]. Alkaloids, terpenoids, steroids, quinolones, isocoumarins, lignans, phenylpropanoids, phenols, and lactones are some of the most common classes of fungal bioactive chemicals [6]. Antimicrobial action against a wide variety of microorganisms has been shown by *Trichoderma* sp., a fungal species present in many habitats [7]. Moreover, *Aspergillus niger* is one of the most well-known fungi, and has been isolated from several niches (soil, nuts and food). Extracellular enzymes and citric acid produced from *A. niger* are known as Generally Recognized As Safe for human consumption (GRAS) by the FDA because of their usage in several industrial settings [8]. Hence, *A. niger* has been considered a valuable resource for the biotechnological sector due to the abundance of secondary metabolites with immunomodulatory and cytotoxic properties against cancer cells [9].

On the other hand, chemically synthesized compounds, namely ionic liquids (ILs), are one of the most interesting scientific and technological advancements for their various applications over the last few decades. There have been significant developments regarding the relevance of these types of unique molecules with adjustable biological and industrial properties [10,11]. Initially, ionic liquids were identified as a combination of inorganic counter anions and organic counter cations. During the synthesis of ionic liquids, the generation of nitrogen-containing heterocyclic molecules contributes significantly [12]. In contrast, hydrazones have become significant molecules in modern chemical synthesis, garnering considerable interest. They were used in a variety of pharmaceuticals and chemotherapeutic drugs [13]. Their attachment to organic molecules plays a crucial role in essential biological processes and in the formulation of medications with a wide range of biological characteristics, including antibacterial [14], anticancer [15], anti-inflammatory [16], antifungal [17], and antitubercular [18] activities. Recently, dicationic ionic liquids (DiILs), a new category of the ILs family, has attracted a great amount of researchers' attention as it represents an interesting variation of the cationic partner. DiILs consist of two head groups (cations) linked by a rigid or flexible spacer and two anions [19].

Hence, the aim of the present study was to synthesize a dicationic pyridinium iodide compound, and characterize and combine it with a biologically active natural product for its potential synergistic effect.

## 2. Results and Discussions

### 2.1. Molecular Identification of Fungal Isolates

In the current study, two endophytic fungal strains were isolated from *Mangifera Indica* roots. The isolates were identified using ITS4 and ITS5 rRNA sequencing. The sequences obtained were compared with the nucleotide sequences of the international database. The isolated fungal strains were *Aspergillus niger* with GenBank accession number MT597434.1 (100% similarity) and *Trichoderma lixii* with GenBank accession number KU324798.1 (98.18% similarity). Furthermore, the phylogenetic tree was generated by performing a distance matrix analysis (Figure 1).

### 2.2. Antibacterial Activity of Fungal Bioactive Secondary Metabolites

Data in Table 1 revealed that the inhibition zones (IZ) diameter of *T. lixii* and *A. niger* crude extracts ranged from 8.0 to 20.0 mm and from 7.5 to 21.0 mm, respectively, against the tested pathogens. *Staphylococcus aureus* and *E. coli* were the most susceptible organisms against *A. niger* and *T. lixii* crude extracts, respectively.

Quang et al. [20] stated that *A. niger* metabolites have been considered as a promising source of antibiotics that inhibit the growth of the Gram-positive bacterium *E. faecalis*, with MIC values ranging from 32 to 64 mM, and of *Candida albicans*, with MIC values ranged from 64 to 128 mM. Meanwhile, Padhi et al. [21] revealed that *A. niger* metabolites showed antifungal activity against *Candida albicans* with IC<sub>50</sub> 31 mg/mL, and antibacterial activity against *Pseudomonas aeruginosa*, *Escherichia coli* and *Staphylococcus aureus* with IC<sub>50</sub> of 160 mg/mL, 47 mg/mL and 135 mg/mL, respectively. Chigozie et al. [22] reported that the fungal extract of *Aspergillus* sp. isolated from fresh leaves of *Mangifera indica*. exhibited antibacterial activity against *P. aeruginosa* and *E. coli*.

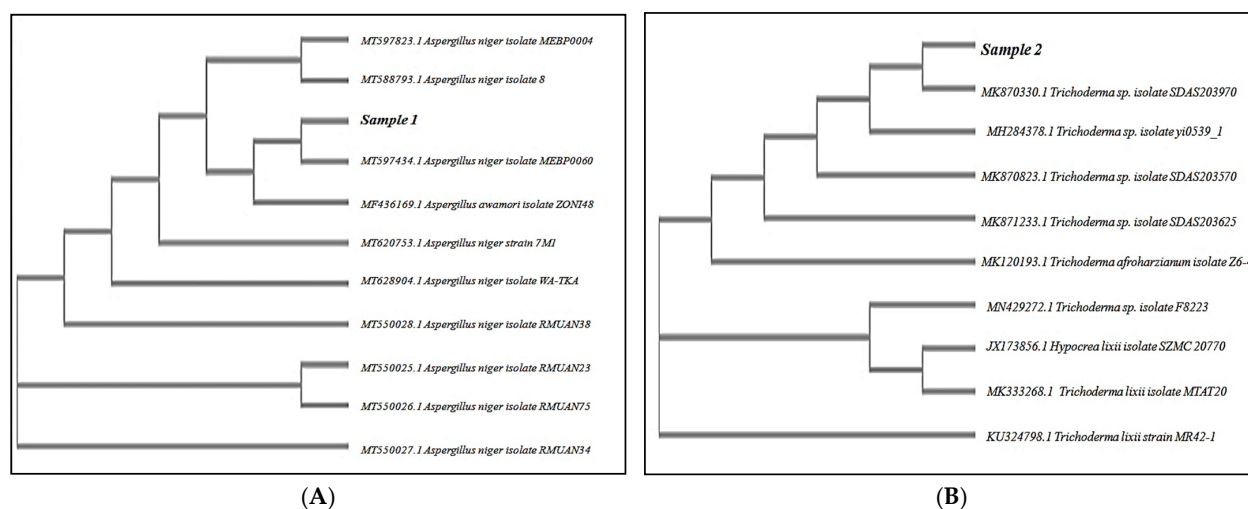


Figure 1. Phylogenetic tree of *A. niger* MT597434.1 (A) and *Trichoderma lixii* KU324798.1 (B).

Table 1. Antibacterial activity of fungal bioactive secondary metabolites against MDR pathogens.

Tested Pathogens	<i>T. lixii</i> Crude Extract			<i>A. niger</i> Crude Extract		
	IZ Diameter (mm)	MIC (µg/mL)	MBC (µg/mL)	IZ Diameter (mm)	MIC (µg/mL)	MBC (µg/mL)
<i>Pseudomonas aeruginosa</i>	14.5	250	500	19.0	250	500
<i>Acinetobacter baumannii</i>	9.0	500	1000	7.5	500	1000
<i>Proteus vulgaris</i>	12.5	250	500	13.0	250	500
<i>Staphylococcus aureus</i>	11.0	500	1000	21.0	250	1000
<i>Escherichia coli</i>	20.0	250	250	12.0	250	250
<i>Klebsiella aerogenes</i>	8.0	500	1000	7.5	1000	1000
<i>Klebsiella pneumoniae</i>	16.0	250	500	11.0	250	500

### 2.3. GC-MS Analysis of Fungal Secondary Metabolites

Data in Figure 2 proved that the *A. niger* crude extract was mainly composed of Pentadecanoic acid, 14-methyl-, methyl ester and 9-Octadecenoic acid (Z)-, and methyl ester (26.66 and 18.01%, respectively). However, the *T. lixii* crude extract's relatively major components were 2,4-Decadienal, (E,E) and 9-Octadecenoic acid (Z)-, and methyl ester (10.69 and 10.32%, respectively) (Table 2). Venice et al. [23] stated that a GC-MS analysis of *T. lixii* crude extract identified the presence of 1,3,3-Trimethyl-Diepoxyhexadecane and 3-Octadecenoic acid compounds. An analysis of endophytes' diversity has determined relationships among host plants and the endophytic fungi, through determining various secondary metabolites biosynthesized from the culture extract of the endophytic fungal isolates [23].

Table 2. Retention time (RT) and probable compounds according to MS library.

Strain	RT	Compound	Area%
<i>A. niger</i>	7.29	1-Octanol, 2,7-dimethyl	6.72
	19.15	2-(Octadecyloxy)ethanol	3.00
	12.74	Pentadecanoic acid, 14-methyl-, methyl ester	26.66
	14.17	9-Octadecenoic acid (Z)-, methyl ester	18.01
<i>T. lixii</i>	7.49	2,4-Decadienal, (E,E)	10.69
	13.36	Undecanoic acid	7.98
	14.59	9-Octadecenoic acid (Z)-, methyl ester	10.32
	16.65	1,2-15,16-Diepoxyhexadecane	7.84
	18.42	Heptadecane, 9hexyl	1.86

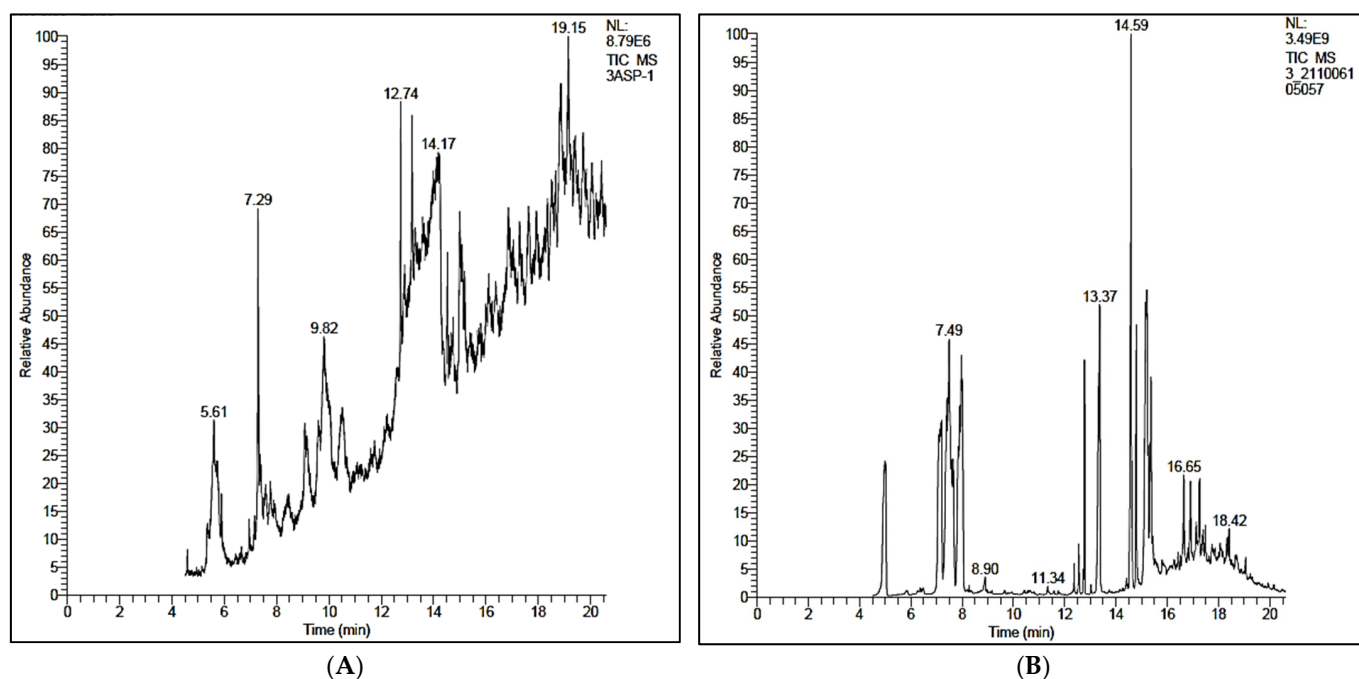


**Figure 2.** GC-MS chromatogram of *Aspergillus niger* (A), and *Trichoderma lixii* (B).

#### 2.4. Molecular Docking Study

Among the most common mechanisms, the Extended-spectrum  $\beta$ -lactamases (ESBLs) were widely reported [24]. One of the main concerns is that resistance caused by these enzymes may result in an efficacy reduction of antimicrobial therapy, or in failed treatment [25]. The reported findings demonstrated that ESBL-variants of SHV-type were the most frequent mechanisms of resistance in ESBL-producing *K. pneumoniae* isolates implicated in bacteremia. Hence, the SHV enzyme was chosen in the present investigation to assess the possible mechanistic action of the synthesized dicationic pyridinium iodide compound, as well as the naturally extracted compounds.

In the current study, molecular docking was performed to predict the binding affinity of the naturally extracted and chemically synthesized compounds toward the target ESBL enzyme SHV-1 (Table 3). The results of the docking studies showed an excellent binding manner with the active site of the target macromolecules, in comparison to the reference drug co-crystallized ligand LN1-255. The naturally extracted compounds showed higher binding scores when compared to the dicationic pyridinium iodide compound ( $-6.38$  kcal/mol), where Pentadecanoic acid, 14-methyl-, methyl ester and 9-Octadecenoic acid (*Z*-), methyl ester (extracted from *Aspergillus niger*) had  $-6.51$  and  $-6.50$  kcal/mol. *Trichoderma lixii*'s most potent compounds were 9-Octadecenoic acid (*Z*-), methyl ester, 1,2-15,16-Diepoxyhexadecane and Heptadecane, 9hexyl, showing  $-6.96$ ,  $-6.56$  and  $-6.99$  kcal/mol binding affinity, respectively. The binding interactions of the dicationic pyridinium iodide compound revealed that the dicationic pyridinium iodide compound was well oriented inside the enzyme pockets and showed hydrophobic interaction with Arg244, Ala280 and Tyr105.

**Table 3.** Binding scores (Kcal/mol) of the investigated molecule with the target SHV-1 enzymes.

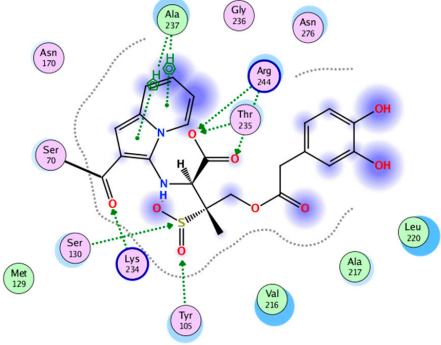
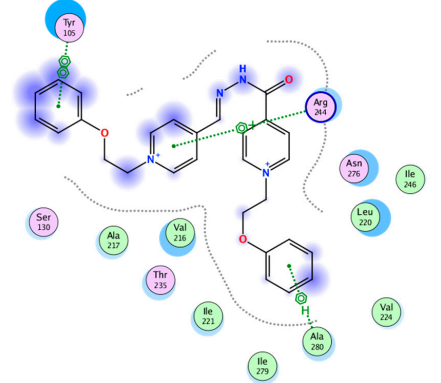
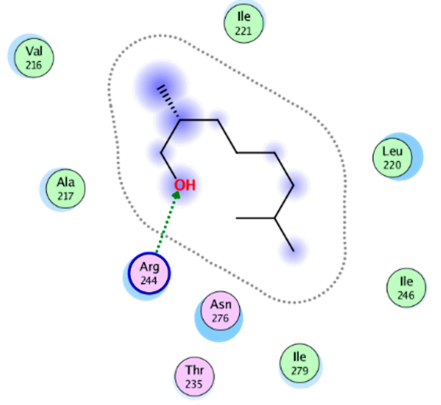
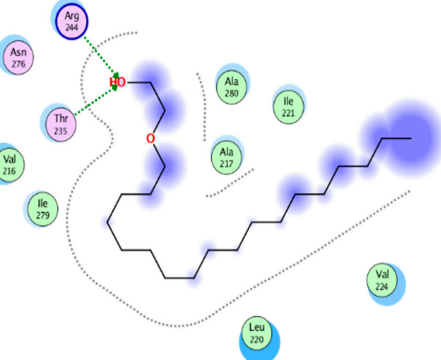
Compounds	Docking Score (kcal/mol)	2D Binding Mode within SHV-1 Active Site
Ref. Co-crystallized ligand LN1-255	−6.44	 <p>The diagram shows the co-crystallized ligand LN1-255 (a complex heterocyclic structure) docked in the SHV-1 active site. It is surrounded by several amino acid residues: Asn 170, Ser 70, Met 129, Lys 234, Tyr 105, Val 216, Thr 235, Arg 244, Gly 236, Asn 276, Ala 217, and Leu 270. Dotted lines indicate hydrogen bonds between the ligand and these residues.</p>
Syn. Comp. Dicationic pyridinium iodide compound	−6.38	 <p>The diagram shows a dicationic pyridinium iodide compound docked in the SHV-1 active site. It is surrounded by residues: Tyr 105, Ser 130, Ala 217, Val 216, Thr 235, Ile 221, Ile 279, Arg 244, Asn 276, Ile 246, Leu 220, Val 224, and Ala 280. Dotted lines indicate interactions between the compound and these residues.</p>
1-Octanol, 2,7-dimethyl	−5.00	 <p>The diagram shows 1-Octanol, 2,7-dimethyl docked in the SHV-1 active site. It is surrounded by residues: Val 216, Ile 221, Ala 217, Arg 244, Asn 276, Thr 235, Ile 279, Leu 220, and Ile 246. Dotted lines indicate interactions between the alcohol and these residues.</p>
<i>A. niger</i>		
2-(Octadecyloxy)ethanol	−6.40	 <p>The diagram shows 2-(Octadecyloxy)ethanol docked in the SHV-1 active site. It is surrounded by residues: Arg 244, Asn 276, Thr 235, Val 216, Ile 279, Ala 280, Ala 217, Ile 221, Val 224, and Leu 220. Dotted lines indicate interactions between the long-chain alcohol and these residues.</p>

Table 3. Cont.

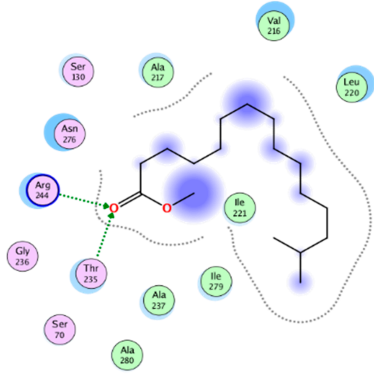
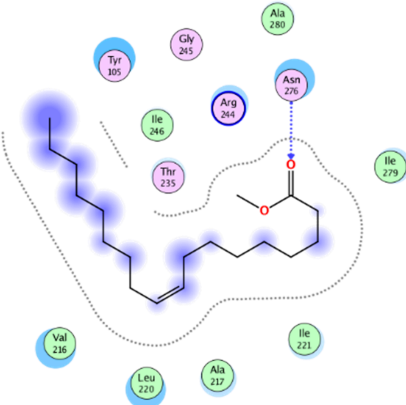
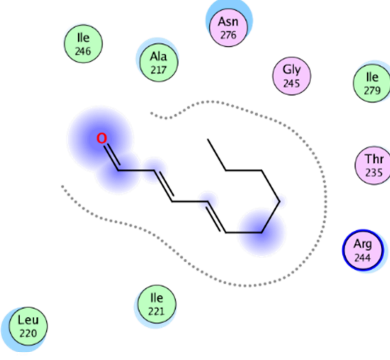
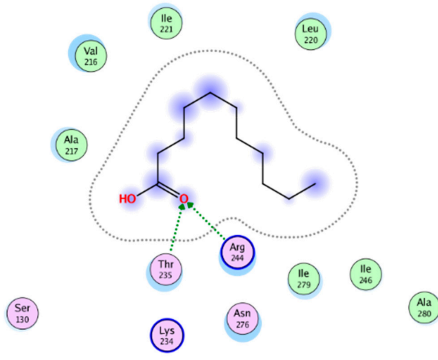
Compounds	Docking Score (kcal/mol)	2D Binding Mode within SHV-1 Active Site
Pentadecanoic acid, 14-methyl-, methyl ester	−6.51	
9-Octadecenoic acid (Z)-, methyl ester	−6.50	
2,4-Decadienal, (E,E)	−5.04	
<i>T. lixii</i>		
Undecanoic acid	−5.62	

Table 3. Cont.

Compounds	Docking Score (kcal/mol)	2D Binding Mode within SHV-1 Active Site
9-Octadecenoic acid (Z)-, methyl ester	−6.96	
1,2-15,16-Diepoxyhexadecane	−6.56	
Heptadecane, 9hexyl	−6.99	

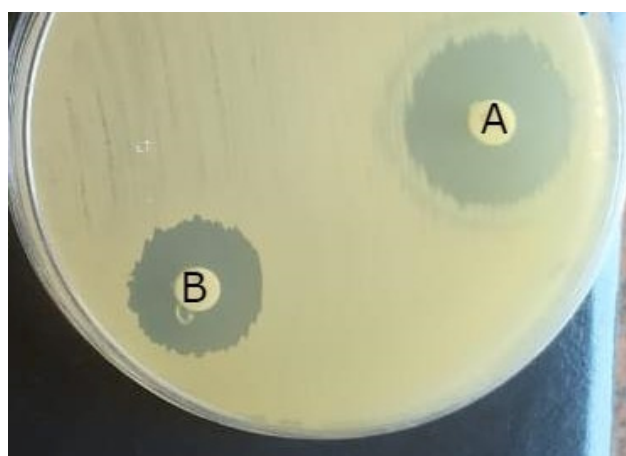
## 2.5. Comparative Study between *T. lixii*, *A. niger* Crude Extracts and Dicationic Pyridinium Iodide Compound

### 2.5.1. Disc Diffusion Technique

Data in Table 4 revealed that the combined action of *A. niger* crude extract with the dicationic pyridinium iodide compound was synergistic against all the tested pathogens except *S. aureus*, while the combined action of *T. lixii* crude extract with dicationic pyridinium iodide was synergistic only against *K. pneumoniae* (Figure 3). Hence, *K. pneumoniae* was selected for further analyses.

**Table 4.** Sensitivity test of *T. lixii* and *A. niger* crude extract in combination with dicationic pyridinium iodide compound.

Tested Pathogens	Dicationic Pyridinium Iodide	IZ Diameter (mm)			
		<i>A. niger</i> Crude Extract	<i>T. lixii</i> Crude Extract	<i>A. niger</i> Crude Extract + Dicationic Pyridinium Iodide	<i>T. lixii</i> Crude Extract + Dicationic Pyridinium Iodide
<i>P. aeruginosa</i>	10.0	19.0	14.5	30.5	14.5
<i>A. baumannii</i>	9.0	7.5	9.0	17.0	9.0
<i>P. vulgaris</i>	10.5	13.0	12.5	24.5	12.5
<i>S. aureus</i>	14.3	21.0	11.0	22.0	16.0
<i>E. coli</i>	13.0	12.0	20.0	34.5	20.0
<i>K. aerogenes</i>	14.0	7.5	8.0	23.0	8.0
<i>K. pneumoniae</i>	12.0	11.0	16.0	24.5	32.0

**Figure 3.** The combined effect of dicationic pyridinium iodide compound with *T. lixii* crude extracts (A) and *A. niger* (B) against *K. pneumoniae*.

### 2.5.2. Checkerboard Dilution Technique

Data in Table 5 proved that the combined actions of the dicationic pyridinium iodide compound with *A. niger* and *T. lixii* crude extracts were synergistic against *K. pneumoniae*, with FICI 0.35 and 0.4, respectively. The observed antibacterial effect was further investigated against *K. pneumoniae* based on the FICI and MIC values.

**Table 5.** Synergy test of *T. lixii* crude extract and *A. niger* crude extract in combination with the dicationic pyridinium iodide compound.

Antibacterial Agent	MIC of Single Drug ( $\mu\text{g/mL}$ )	MIC of Combined Drug ( $\mu\text{g/mL}$ )	FIC	FICI	Interpretation	
<i>K. pneumoniae</i>	dicationic pyridinium iodide	250.0	50.0	0.20	-	-
	<i>A. niger</i> crude extract	250.0	37.5	0.15	0.35	Synergy
	<i>T. lixii</i> crude extract	250.0	50.0	0.20	0.4	Synergy

–: Not detected.

### 2.6. Mechanistic Action of the Combined Formula

Transmission electron microscopic (TEM) study was applied to the treated cells of *K. pneumoniae* against the combined drugs (*A. niger*/dicationic pyridinium iodide and *T. lixii*/dicationic pyridinium iodide). Figure 4 revealed a breakage in the cell wall and deformation of the cells, with leakage of the intracellular components that lead to cell death. Moreover, *A. niger*/dicationic pyridinium iodide and *T. lixii*/dicationic pyridinium



iodide combined drugs showed potent antibacterial activity by inhibiting the bacterial growth after 6 and 4 h, respectively (Figure 5). Moreover, the reactive oxygen species (ROS) study of the treated bacterial cells revealed that by increasing the formula concentration the ROS increased, which elaborated the cell membrane damage and reduced bacterial cells' viability (Figure 6).

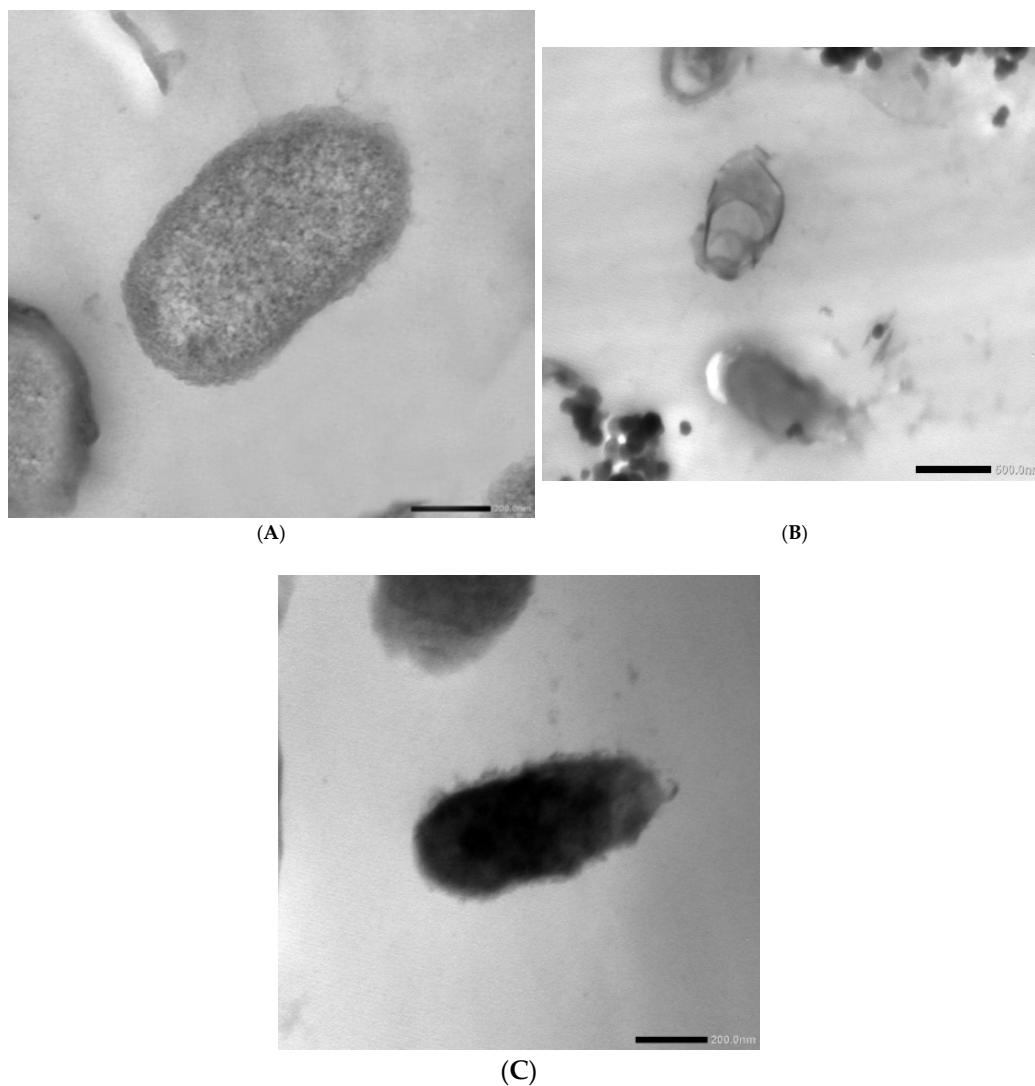


**Figure 4.** Transmission electron microscopic micrograph of *K. pneumoniae* untreated control (A), *T. Lixii*/dicationic pyridinium iodide (B) and *A. niger*/dicationic pyridinium iodide (C) treated cells.

Guo et al. [26] studied the antibacterial activity of *Aspergillus niger* crude extract (fraction B10) against *Agrobacterium tumefaciens* T-37 with an inhibition percentage of 98.22%, and the dose required to achieve 50% inhibition was 0.035–0.018 mg/mL. The antibacterial mechanism was evaluated by using electric conductivity, the release of proteins and nucleic acids, sodium dodecyl sulphate–polyacrylamide gel electrophoresis (SDS–PAGE), and the detection of reactive oxygen species (ROS). An increase in the relative electric conductivity of the supernatant was noticed with the addition of *Aspergillus niger* crude extract B10, which indicated that there was electrolyte transfer from the intracellular to the extracellular matrix. In contrast to the control group, the B10 fraction treated group showed a high increase in the amount of extracellular nucleic acid and protein between 0 and 18 h, and damage in the cytoplasmic membranes was noticed. SDS–PAGE analysis showed that the amounts of extracellular protein and nucleic acid were consistent with the lower levels of total protein inside the cells. It was demonstrated that B10 was responsible for the rise in ROS.

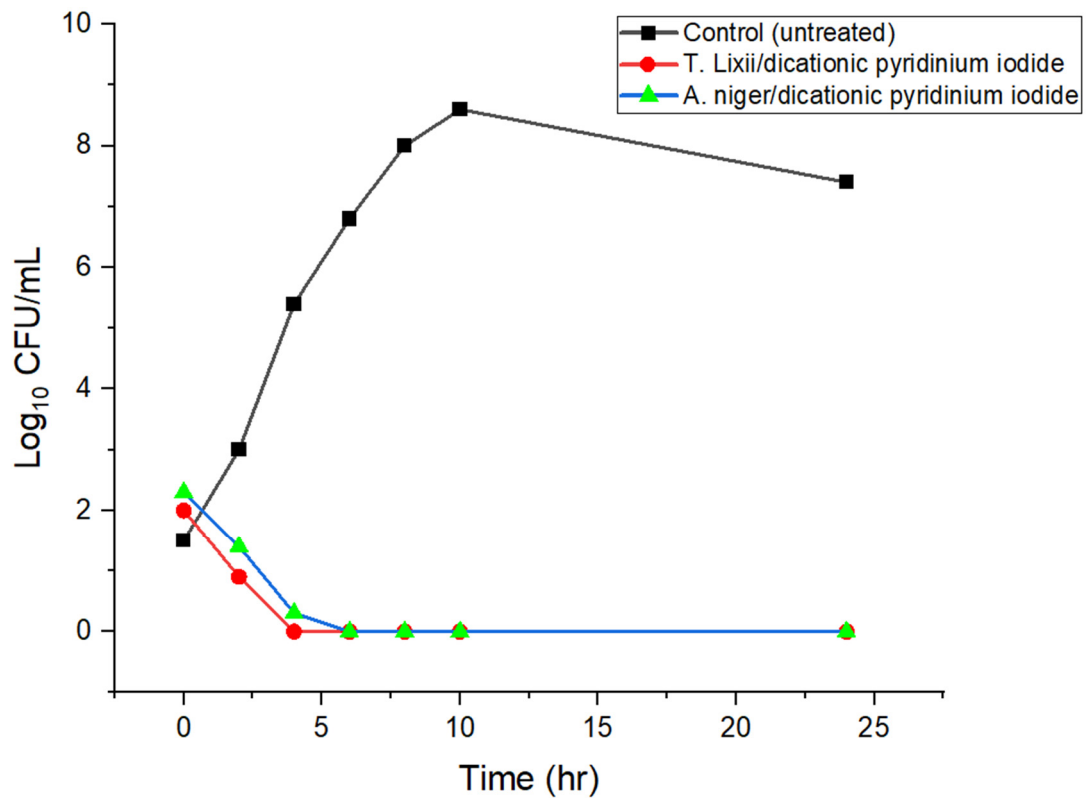


Figure 5. Bacterial growth in the presence and absence of the combined formulae.

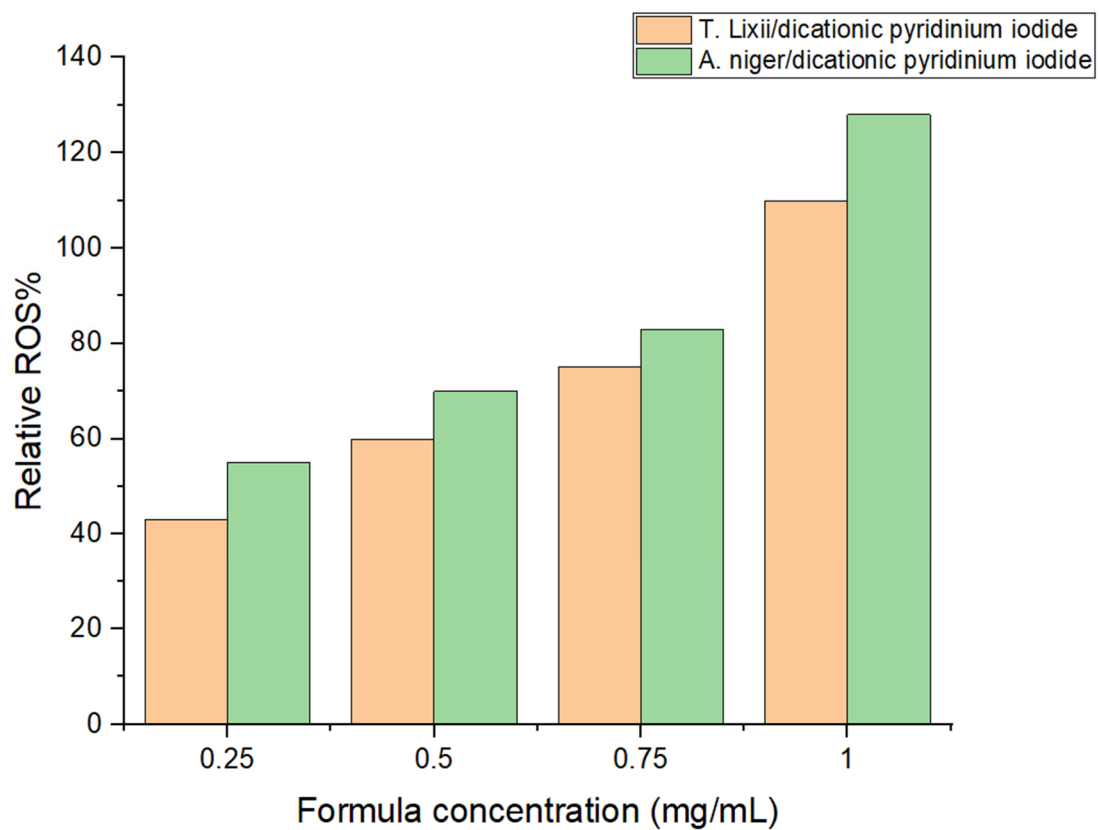


Figure 6. ROS production in the presence of the combined formulae.

On the other hand, Qiao et al. [27] revealed that aspermerodione extracted from the endophytic fungus *Aspergillus* sp. TJ23 showed a synergistic effect with  $\beta$ -lactam antibiotics oxacillin and piperacillin as potent antibacterial combinations against MRSA. It was reported that combination therapy can be used as a promising strategy for combatting MRSA through extending the lifespan and efficacy of the currently employed antibiotics. The present investigation may pave the way into combating microbial infections through natural/synthetic combinations.

### 3. Materials and Methods

#### 3.1. Tested Pathogens

*Pseudomonas aeruginosa*, *Acinetobacter baumannii*, *Proteus vulgaris*, *Staphylococcus aureus*, *Escherichia coli*, *Klebsiella aerogenes* and *Klebsiella pneumoniae* were kindly provided and identified by El-Shatby pediatric hospital using the Vitek 2 automated system (bioMerieux, Marcy l'Etoile, France) at the Medical Research Center, Faculty of Medicine, Alexandria University. The tested pathogens were kept in brain–heart infusion glycerol broth at  $-4\text{ }^{\circ}\text{C}$  for further investigations, with monthly transfer into fresh media. The tested pathogens were identified as multi-drug resistant according to CLSI guidelines (Table S1).

#### 3.2. Endophytic Fungal Isolation

Fungal samples were isolated from the roots of fully matured and healthy plants of *Mangifera Indica* at El Nubaria, Alexandria ( $30^{\circ}41'57''\text{ N}$ ,  $30^{\circ}40'1''\text{ E}$ ), with firm leaves and well-formed fruits, leaves and root systems. The root samples were rinsed with running tap water followed by deionized water and subsequently dipped in 70% ethanol (1–2 min), followed by sterilization in 0.1% sodium hypochlorite (2–3 min). They were further dipped in 70% ethanol and finally rinsed with distilled water. The roots were allowed to dry, and were cut aseptically into small pieces ( $1\text{ cm}^2$ ) and patched onto potato dextrose agar (PDA) (Himedia, Mumbai, India) plates containing streptomycin (SRL, Mumbai, India) at a concentration of  $250\text{ }\mu\text{g/mL}$  to prevent bacterial contamination [28].

#### 3.3. Molecular Identification of the Fungal Isolates

Fungal isolates were identified through ITS based DNA sequencing using the conserved ITS region of fungal gDNA amplified by general primers ITS4 (5'-TCCTCCGCTTA TTGATATGC-3') and ITS5 (5'-GGAAGTAAAAGTCGTAACAAGG-3'). ITS sequences of the identified fungi were submitted to GenBank for the retrieval of their accession numbers [28]. The study of percentage identity of the aligned sequences was carried out using a Kolmogorov–Smirnov statistical test in GeneDoc (version 2.7). Using the obtained sequences, phylogenetic analysis was performed and a phylogenetic tree was constructed through MEGA (v10.1.8) by the maximum likelihood Bootstrap (MLBS) method.

#### 3.4. Seed Culture Preparations and Extraction of Fungal Secondary Metabolites

Spore suspension seed cultures were prepared according to CLSI guidelines [29]. Fungal isolates were inoculated (mycelial plugs ( $1 \times 1\text{ cm}^2$ )) into 300 mL potato-dextrose broth then incubated for 21 days at  $25\text{ }^{\circ}\text{C}$  under shaken conditions (140 rpm). At the end of the incubation period, the mycelia were harvested through filtration and the filtrate was extracted with chloroform/methanol (2:1, v/v) for 4 h. The crude fungal extract containing the bioactive compounds was stored at  $4\text{ }^{\circ}\text{C}$  for further experimental processes [28].

#### 3.5. Antibacterial Activity of Fungal Secondary Metabolites

Antibacterial activity was carried out using the disc-diffusion method; the discs were saturated with  $25\text{ }\mu\text{L}$  of each fungal extract ( $20\text{ mg/mL}$ ) and placed on the surface of inoculated Müller–Hinton agar plates [30]. Further antibacterial activity evaluation was carried out by assessing the minimal inhibitory concentration (MIC) and minimum bactericidal concentration (MBC) values [31]. MIC and MBC evaluations were performed through mixing  $80\text{ }\mu\text{L}$  of sterile Müller–Hinton broth,  $20\text{ }\mu\text{L}$  tween 80, and  $100\text{ }\mu\text{L}$  of the

fungus secondary metabolites one at a time. The mixture was then diluted serially using a two-fold dilution in a 96-well microtiter plate. Then, 100  $\mu\text{L}$  of 0.5 McFarland of the tested bacterial suspensions was inoculated in each well. MIC is the minimum concentration of the tested drugs that inhibited the bacterial growth, while the MBC is the minimum concentration needed to completely kill the microbial cells [32].

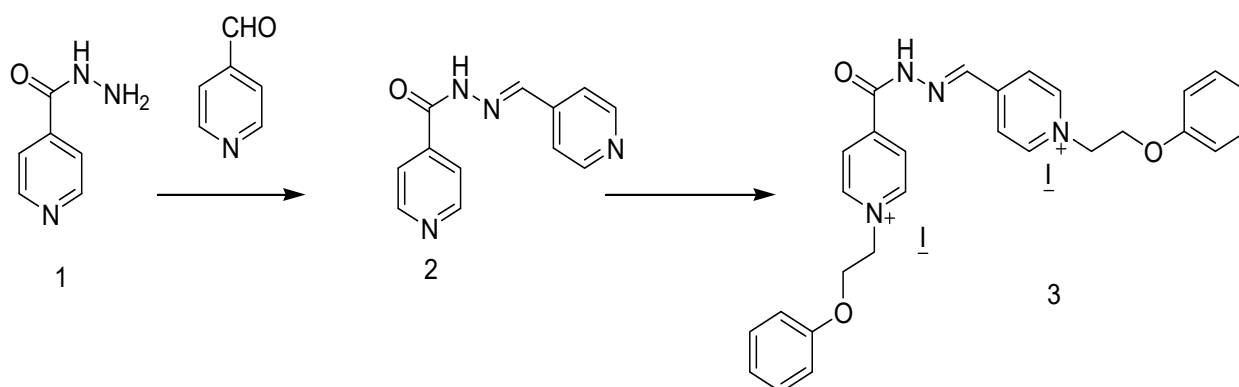
### 3.6. GC-MS Analysis of Fungal Secondary Metabolites

For the GC-MS analysis, 2  $\mu\text{L}$  of samples were injected into the GC-MS device equipped with a splitless injector and a PE Auto system XL gas chromatograph interfaced with a Turbo-mass spectrometric mass selective detector system. The MS was operated in the EI mode (70 eV) with helium as the carrier gas (flow rate 1 mL/min) and an analytical column HP (length 30 mm–0.20 mm, 0.11 mm film thickness). The MS was operated in the total ion current (TIC) mode, scanning from  $m/z$  30 to 400. The bioactive compounds were identified by comparing their retention time (RT in min) and mass spectra with the library of the National Institute of Standards and Technology (NIST), USA [33].

### 3.7. Chemical Synthesis of Dicationic Pyridinium Iodide Compounds

A mixture of 4-pyridinecarboxaldehyde (10 mmol) in ethanol (30 mL) and isonicotinic acid hydrazide (1) (10 mmol) with a few drops of hydrochloric acid was heated under reflux for 1 h. The solid obtained after the solvent evaporation under pressure was recrystallized from ethanol to furnish the desired Schiff base 2.

The 4(2-iodoethoxy)benzene (10 mmol) was added under stirring to a solution of dipyridine Schiff base 2 (5 mmol) in acetonitrile (30 mL). Then, the reaction mixture was heated under reflux for 8 h, until the consumption of the starting material was indicated by TLC (silica gel, hexane-ethyl acetate). The solvent was reduced by evaporation under reduced pressure; the product formed was collected by filtration to afford the desired dicationic pyridinium iodide (3) (Scheme 1) [19].



**Scheme 1.** Chemical synthesis of dicationic pyridinium iodide compound.

#### 3.7.1. Characterization of the Prepared Dicationic Pyridinium Iodide (3)

mp: 82–83 °C.  $^1\text{H}$  NMR (400 MHz, DMSO- $d_6$ ):  $\delta_{\text{H}}$  = 4.54 (t, 4H,  $J$  = 8 Hz,  $2 \times \text{NCH}_2$ ), 5.18 (t, 4H,  $J$  = 8 Hz,  $2 \times \text{OCH}_2$ ), 6.94–6.96 (m, 6H, Ar-H), 7.31 (dd, 4H,  $J$  = 4 Hz, 8 Hz, Ar-H), 8.24 (d, 0.5H,  $J$  = 4 Hz, Ar-H), 8.33 (d, 0.5H,  $J$  = 4 Hz, Ar-H), 8.48 (d, 1.5H,  $J$  = 4 Hz, Ar-H), 8.63 (d, 1.5H,  $J$  = 4 Hz, Ar-H), 8.71 (s, 0.75H, H-C-N), 8.84 (s, 0.25H, H-C-N), 9.08 (d, 0.5H,  $J$  = 4 Hz, Ar-H), 9.22 (d, 1.5H,  $J$  = 4 Hz, Ar-H), 9.35 (d, 0.5H,  $J$  = 4 Hz, Ar-H), 9.45 (d, 1.5H,  $J$  = 4 Hz, Ar-H), 12.89 (s, 0.25H, CONH), 13.28 (s, 0.75H, CONH).  $^{13}\text{C}$  NMR (100 MHz, DMSO- $d_6$ ):  $\delta_{\text{C}}$  = 60.22, 60.90 ( $2 \times \text{NCH}_2$ ), 66.43, 66.54 ( $2 \times \text{OCH}_2$ ), 115.11, 121.94, 125.19, 126.76, 130.08, 144.95, 146.38, 147.05, 147.51, 149.69 (Ar-C), 157.93, 160.34 (C=N, C=O)

### 3.7.2. Molecular Docking

The crystal structure of SHV-1  $\beta$ -lactamase (Pdb: 3D4F), available at RCSB Protein Data Bank, was used as a template for constructing the 3D models [34].

#### Database Generation and Optimization

The ChemDraw application was used to draw the test compounds, and the MOE software database was utilized to gather these compounds once they had been drawn. Displaying hydrogen, computing partial charges, and using the default energy minimization were the three methods that were used in the optimization of the database. After the triangular matcher algorithm ligand was applied to the setting of the ligand placement, the default scoring function was employed to obtain the top five non-redundant poses that had the lowest binding energy of the test compound. In order to record the most effective potential molecular interactions, the docking of the optimized database was carried out using the induced fitting methodology. The docking score, expressed in Kcal/mol, was determined by combining the results of two different scoring functions—namely, alpha hydrogen bonding and London dG forces. The acquired results were organized into a list based on the S-scores that had an RMSD value of less than 2. The correctness of the employed software is heavily reliant on the training set, and the results of the molecular docking may be confirmed using a training set of experimental ligand–protein complexes. In order to guarantee a genuine and dependable docking strategy, the software that is being used needs to be able to reproduce the binding mode of an established reference inhibitor for the enzyme that is being targeted. The co-crystallized ligand LN1-255 was chosen as the comparison standard for the docking study in the experiment as a positive control (reference values). In the end, conformers that had the greatest binding scores and the best ligand–enzyme interactions were detected and examined [35].

### 3.8. Combination Study between the Fungal Extracts and the Synthesized Dicationic Pyridinium Iodide Compound

Combination studies were carried out according to White et al. [36]. The disc diffusion method was used to assess the possible differences in the inhibition zone diameter upon mixing the fungal extracts and the synthesized dicationic pyridinium iodide compound (1:1 *w/w*). Furthermore, the broth microdilution checkerboard technique was employed to study the synergistic effect between the fungal extract (Agent A) and dicationic pyridinium iodide compound (Agent B). Two-fold serial dilutions of the fungal extract and dicationic pyridinium iodide compound were dispensed in a 96-well microtiter plate with sub-MIC concentration. A 100  $\mu$ L quantity of the bacterial suspension ( $1.5 \times 10^6$  CFU/mL) was dispensed into each well and incubated for 24 h at  $35 \pm 2$  °C. The fractional inhibitory concentration index (FICI) was computed, with the following equation:

$$\text{FICI} = \text{FIC of agent A} + \text{FIC of agent B}$$

where

$$\text{FIC of agent A} = \frac{\text{MIC of antimicrobial agent A in combination}}{\text{MIC of antimicrobial agent A alone}}$$

$$\text{FIC of agent B} = \frac{\text{MIC of antimicrobial agent B in combination}}{\text{MIC of antimicrobial agent B alone}}$$

FICI was considered as synergistic when it was  $\leq 0.5$ , and as additive when it was  $>0.5-1$ , indifferent when it was  $\geq 1-4.0$  and antagonistic when it was  $>4$  [31].

### 3.9. Antibacterial Mechanism of Action of the Combined Formulae

#### 3.9.1. Transmission Electron Microscopic (TEM) Examination of the Treated Microbial Cells

On the basis of FIC and FICI values, the most susceptible bacterial strain (*K. pneumoniae*) was treated with the combined drugs. Samples were fixed using a universal electron microscope fixative. A series of dehydration steps were followed using ethanol and propy-

lene oxide. The samples were then embedded in labeled beam capsules and polymerized. Thin sections of cells exposed to extracts were cut using LKB 2209-180 ultra-microtome and stained with a saturated solution of uranyl acetate for half an hour and lead acetate for 2 min [31]. Electron Micrographs were taken using a Transmission Electron Microscope (JEM-100 CX Joel).

### 3.9.2. Time-Kill Curve

A time-kill curve was investigated to estimate the optimum time required to inhibit the bacterial vegetative cells. Fungal secondary metabolites combined with the dicationic pyridinium iodide compound (FIC and FICI values of each) were added one at a time to 10 mL Müller–Hinton broth containing  $1 \times 10^6$  CFU/mL bacterial cells. Aliquots were withdrawn to assess the bacterial growth through different incubation time (0, 2, 4, 6, 8, 12 and 24 h) at OD 600 nm [37].

### 3.9.3. Reactive Oxygen Species (ROS) Study

The reactive oxygen species (ROS) generation assay was measured according to Almo-tairy et al. [38] and Bhuvaneshwari et al. [39] using 2,7-dichlorofluorescein diacetate (DCFH-DA) dye by comparing the extracellular ROS of the treated and control bacterial cells.

## 4. Conclusions

In the current study, two endophytic fungal strains with antimicrobial activities were isolated from *Mangifera Indica* roots and identified as *Aspergillus niger* MT597434.1 and *Trichoderma lixii* KU324798.1. A dicationic pyridinium iodide compound was synthesized and then evaluated for its potential synergistic effect with the extracted fungal crude extract. The molecular modeling study revealed that the synthesized dicationic pyridinium iodide compound and the extracted fungal secondary metabolites showed promising inhibitory effects against the SHV-1 enzyme. The combination of *A. niger* and *T. lixii* secondary metabolites with the dicationic pyridinium iodide compound showed a synergistic effect against *K. pneumoniae*. Fungal secondary metabolites combined drugs inhibited the bacterial growth after 6 and 4 h through cell wall breakage and cells' deformation with intracellular components leakage and increased ROS production, which led to bacterial cell death. This study proved the importance of the combination of fungal secondary metabolites and some synthetic drugs against multi-drug resistant microbial cells through several modes of action, which may pave the way to more available naturally derived options.

**Supplementary Materials:** The following supporting information can be downloaded at: <https://www.mdpi.com/article/10.3390/molecules28062434/s1>, Table S1: The resistance prevalence in the tested pathogens.

**Author Contributions:** Conceptualization, B.H.E., M.H. and Z.A.O.; methodology, A.M.A.; software, M.Z.M.; validation, B.H.E.; formal analysis, M.H.; investigation, B.H.E.; resources, Z.A.O.; data curation, B.H.E. and A.M.A.; writing—original draft preparation, B.H.E., A.M.A., Z.A.O. and M.H.; writing—review and editing, B.H.E. and Z.A.O.; visualization, A.M.A.; supervision, B.H.E., M.Z.M., M.H. and Z.A.O. All authors have read and agreed to the published version of the manuscript.

**Funding:** This research received no external funding.

**Institutional Review Board Statement:** Not applicable.

**Informed Consent Statement:** Not applicable.

**Data Availability Statement:** The datasets analyzed during the current study are available from the National Center for Biotechnology Information (NCBI) database (accessed on December 2021).

**Acknowledgments:** We would like to thank Marwa M. Shaaban for helping the student in conducting the molecular docking study during the present study.

**Conflicts of Interest:** The authors declare no conflict of interest.

**Sample Availability:** Not Available.

## References

1. Peyclit, L.; Yousfi, H.; Rolain, J.M.; Bittar, F. Drug repurposing in medical mycology: Identification of compounds as potential antifungals to overcome the emergence of multidrug-resistant fungi. *Pharmaceuticals* **2021**, *14*, 488.
2. Miryala, S.K.; Anbarasu, A.; Ramaiah, S. Role of SHV-11, a class  $\beta$ -lactamase, gene in multidrug resistance among *Klebsiella pneumoniae* strains and understanding its mechanism by gene network analysis. *Microb. Drug Resist.* **2020**, *26*, 900–908. [PubMed]
3. Kandasamy, G.D.; Kathirvel, P. Insights into bacterial endophytic diversity and isolation with a focus on their potential applications—A review. *Microbiol. Res.* **2022**, *266*, 127256. [PubMed]
4. Du, W.; Yao, Z.; Li, J.; Sun, C.; Xia, J.; Wang, B.; Shi, D.; Ren, L. Diversity and antimicrobial activity of endophytic fungi isolated from *Securinega suffruticosa* in the Yellow River Delta. *PLoS ONE* **2020**, *15*, e0229589.
5. Nischitha, R.; Shivanna, M.B. Antimicrobial activity and metabolite profiling of endophytic fungi in *Digitaria bicornis* (Lam) Roem. and Schult. and *Paspalidium flavidum* (Retz.) A. Camus. *3 Biotech* **2021**, *11*, 53.
6. Mao, Z.; Zhang, W.; Wu, C.; Feng, H.; Peng, Y.; Shahid, H.; Cui, Z.; Ding, P.; Shan, T. Diversity and antibacterial activity of fungal endophytes from *Eucalyptus exserta*. *BMC Microbiol.* **2021**, *21*, 155.
7. Ślizewska, W.; Struszczyk-Świta, K.; Marchut-Mikołajczyk, O. Metabolic Potential of Halophilic Filamentous Fungi—Current Perspective. *Int. J. Mol. Sci.* **2022**, *23*, 4189. [PubMed]
8. Torres, A.B.; Bedoya, K.V.; Guerra, J.D.; Montoya-Estrada, C.N.; Castro-Ríos, K. Ultraviolet radiation and generally recognized as safe (GRAS) preservatives for inactivation of *Aspergillus niger* in vitro and corn dough. *Braz. J. Food Technol.* **2022**, *25*, 1–8. [CrossRef]
9. Devi, R.; Kaur, T.; Guleria, G.; Rana, K.L.; Kour, D.; Yadav, N.; Yadav, A.N.; Saxena, A.K. Fungal secondary metabolites and their biotechnological applications for human health. In *New and Future Developments in Microbial Biotechnology and Bioengineering*; Elsevier: Amsterdam, The Netherlands, 2020; pp. 147–161.
10. MacFarlane, D.R.; Kar, M.; Pringle, J.M. *Fundamentals of Ionic Liquids: From Chemistry to Applications*; John Wiley & Sons: Hoboken, NJ, USA, 2017.
11. Zhuang, W.; Hachem, K.; Bokov, D.; Ansari, M.J.; Nakhjiri, A.T. Ionic liquids in pharmaceutical industry: A systematic review on applications and future perspectives. *J. Mol. Liq.* **2021**, *349*, 118145.
12. Ali, I.; Nadeem Lone, M.; AAl-Othman, Z.; Al-Warthan, A.; Marsin Sanagi, M. Heterocyclic scaffolds: Centrality in anticancer drug development. *Curr. Drug Targets* **2015**, *16*, 711–734. [CrossRef]
13. Verma, G.; Marella, A.; Shaquiquzzaman, M.; Akhtar, M.; Ali, M.R.; Alam, M.M. A review exploring biological activities of hydrazones. *J. Pharm. Bioallied Sci.* **2014**, *6*, 69. [PubMed]
14. Bayrak, H.; Demirbas, A.; Demirbas, N.; Karaoglu, S.A. Synthesis of some new 1, 2, 4-triazoles starting from isonicotinic acid hydrazide and evaluation of their antimicrobial activities. *Eur. J. Med. Chem.* **2009**, *44*, 4362–4366. [PubMed]
15. Rezki, N.; Al-Yahyawi, A.M.; Bardaweel, S.K.; Al-Blewi, F.F.; Aouad, M.R. Synthesis of novel 2,5-disubstituted-1,3,4-thiadiazoles clubbed 1,2,4-triazole, 1,3,4-thiadiazole, 1,3,4-oxadiazole and/or Schiff base as potential antimicrobial and antiproliferative agents. *Molecules* **2015**, *20*, 16048–16067.
16. Abdelgawad, M.A.; Labib, M.B.; Abdel-Latif, M. Pyrazole-hydrazone derivatives as anti-inflammatory agents: Design, synthesis, biological evaluation, COX-1, 2/5-LOX inhibition and docking study. *Bioorganic Chem.* **2017**, *74*, 212–220.
17. Moustafa, G.; Khalaf, H.; Naglah, A.; Al-Wasidi, A.; Al-Jafshar, N.; Awad, H. Synthesis, molecular docking studies, in vitro antimicrobial and antifungal activities of novel dipeptide derivatives based on N-(2-(2-hydrazinyl-2-oxoethylamino)-2-oxoethyl)-nicotinamide. *Molecules* **2018**, *23*, 761.
18. Oliveira, P.F.; Guidetti, B.; Chamayou, A.; André-Barrès, C.; Madacki, J.; Korduláková, J.; Mori, G.; Silvia Orena, B.; Chiarelli, L.R.; Pasca, M.R.; et al. Mechanochemical synthesis and biological evaluation of novel isoniazid derivatives with potent antitubercular activity. *Molecules* **2017**, *22*, 1457. [PubMed]
19. Rezki, N.; Al-Sodies, S.A.; Ahmed, H.E.; Ihmaid, S.; Messali, M.; Ahmed, S.; Aouad, M.R. A novel dicationic ionic liquids encompassing pyridinium hydrazone-phenoxy conjugates as antimicrobial agents targeting diverse high resistant microbial strains. *J. Mol. Liq.* **2019**, *284*, 431–444.
20. Quang, T.H.; Phong, N.V.; Anh, L.N.; Hanh, T.T.H.; Cuong, N.X.; Ngan, N.T.T.; Minh, C.V. Secondary metabolites from a peanut-associated fungus *Aspergillus niger* IMBC-NMTP01 with cytotoxic, anti-inflammatory, and antimicrobial activities. *Nat. Prod. Res.* **2022**, *36*, 1215–1223. [PubMed]
21. Padhi, S.; Masi, M.; Panda, S.K.; Luyten, W.; Cimmino, A.; Tayung, K.; Evidente, A. Antimicrobial secondary metabolites of an endolichenic *Aspergillus niger* isolated from lichen thallus of *Parmotrema ravum*. *Nat. Prod. Res.* **2020**, *34*, 2573–2580.
22. Chigozie, V.U.; Okezie, M.U.; Ajaegbu, E.E.; Okoye, F.B.; Esimone, C.O. Bioactivities and HPLC analysis of secondary metabolites of a morphologically identified endophytic *Aspergillus* fungus isolated from *Mangifera indica*. *Nat. Prod. Res.* **2021**, *36*, 5884–5888.
23. Venice, F.; Davolos, D.; Spina, F.; Poli, A.; Prigione, V.P.; Varese, G.C.; Ghignone, S. Genome sequence of *Trichoderma lixii* MUT3171, a promising strain for mycoremediation of PAH-contaminated sites. *Microorganisms* **2020**, *8*, 1258. [CrossRef]
24. Aires-de-Sousa, M.; Lopes, E.; Gonçalves, M.L.; Pereira, A.L.; Machado e Costa, A.; de Lencastre, H.; Poirel, L. Intestinal carriage of extended-spectrum beta-lactamase-producing Enterobacteriaceae at admission in a Portuguese hospital. *Eur. J. Clin. Microbiol. Infect. Dis.* **2020**, *39*, 783–790. [CrossRef] [PubMed]

25. Carvalho, I.; Chenouf, N.S.; Carvalho, J.A.; Castro, A.P.; Silva, V.; Capita, R.; Alonso-Calleja, C.; Enes Dapkevicius, M.D.L.N.; Igrejas, G.; Torres, C.; et al. Multidrug-resistant *Klebsiella pneumoniae* harboring extended spectrum  $\beta$ -lactamase encoding genes isolated from human septicemias. *PLoS ONE* **2021**, *16*, e0250525. [[CrossRef](#)] [[PubMed](#)]
26. Guo, K.; Zhang, Q.; Zhao, J.; Li, Z.; Ran, J.; Xiao, Y.; Zhang, S.; Hu, M. Antibacterial mechanism of *Aspergillus niger* xj spore powder crude extract B10 against *Agrobacterium tumefaciens* T-37. *Biotechnol. Biotechnol. Equip.* **2021**, *35*, 162–169. [[CrossRef](#)]
27. Qiao, Y.; Zhang, X.; He, Y.; Sun, W.; Feng, W.; Liu, J.; Hu, Z.; Xu, Q.; Zhu, H.; Zhang, J.; et al. Aspermerodione, a novel fungal metabolite with an unusual 2, 6-dioxabicyclo [2.2. 1] heptane skeleton, as an inhibitor of penicillin-binding protein 2a. *Sci. Rep.* **2018**, *8*, 5454. [[CrossRef](#)]
28. Verma, A.; Gupta, P.; Rai, N.; Tiwari, R.K.; Kumar, A.; Salvi, P.; Kamble, S.C.; Kumar Singh, S.; Gautam, V. Assessment of biological activities of fungal endophytes derived bioactive compounds Isolated from *Amoora rohituka*. *J. Fungi* **2022**, *8*, 285. [[CrossRef](#)] [[PubMed](#)]
29. Clinical and Laboratory Standards Institute. Performance Standards for Antimicrobial Susceptibility Testing. CLSI Supplement M100. 2017. Available online: [https://clsi.org/media/1795/catalog2017\\_web.pdf](https://clsi.org/media/1795/catalog2017_web.pdf) (accessed on 1 January 2018).
30. Diab, S.E.; Tayea, N.A.; Elwakil, B.H.; Gad, A.A.E.M.; Ghareeb, D.A.; Olama, Z.A. Novel Amoxicillin-Loaded Sericin Biopolymeric Nanoparticles: Synthesis, Optimization, Antibacterial and Wound Healing Activities. *Int. J. Mol. Sci.* **2022**, *23*, 11654. [[CrossRef](#)]
31. Elnaggar, Y.S.; Elwakil, B.H.; Elshewemi, S.S.; El-Naggar, M.Y.; Bekhit, A.A.; Olama, Z.A. Novel Siwa propolis and colistinintegrated chitosan nanoparticles: Elaboration; in vitro and in vivo appraisal. *Nanomedicine* **2020**, *15*, 1269–1284. [[CrossRef](#)]
32. Aljohani, F.S.; Hamed, M.T.; Bakr, B.A.; Shahin, Y.H.; Abu-Serie, M.M.; Awaad, A.K.; El-Kady, H.; Elwakil, B.H. In vivo bio-distribution and acute toxicity evaluation of greenly synthesized ultra-small gold nanoparticles with different biological activities. *Sci. Rep.* **2022**, *12*, 6269. [[CrossRef](#)]
33. Elnahas, R.A.; Elwakil, B.H.; Elshewemi, S.S.; Olama, Z.A. Egyptian *Olea europaea* leaves bioactive extract: Antibacterial and wound healing activity in normal and diabetic rats. *J. Tradit. Complement. Med.* **2021**, *11*, 427–434. [[CrossRef](#)]
34. Shaaban, M.M.; Ragab, H.M.; Akaji, K.; McGeary, R.P.; Bekhit, A.E.A.; Hussein, W.M.; Kurz, J.L.; Elwakil, B.H.; Bekhit, S.A.; Ibrahim, T.M.; et al. Design, synthesis, biological evaluation and in silico studies of certain aryl sulfonyl hydrazones conjugated with 1, 3-diaryl pyrazoles as potent metallo- $\beta$ -lactamase inhibitors. *Bioorganic Chem.* **2020**, *105*, 104386. [[CrossRef](#)] [[PubMed](#)]
35. Al-Humaidi, J.Y.; Shaaban, M.M.; Rezki, N.; Aouad, M.R.; Zakaria, M.; Jaremko, M.; Hagar, M.; Elwakil, B.H. 1, 2, 3-Triazole-Benzofused Molecular Conjugates as Potential Antiviral Agents against SARS-CoV-2 Virus Variants. *Life* **2022**, *12*, 1341. [[CrossRef](#)]
36. White, R.L.; Burgess, D.S.; Manduru, M.; Bosso, J.A. Comparison of three different in vitro methods of detecting synergy: Time-kill, checkerboard, and E test. *Antimicrob. Agents Chemother.* **1996**, *40*, 1914–1918. [[CrossRef](#)] [[PubMed](#)]
37. Wang, D.; Xue, B.; Wang, L.; Zhang, Y.; Liu, L.; Zhou, Y. Fungus-mediated green synthesis of nano-silver using *Aspergillus sydowii* and its antifungal/antiproliferative activities. *Scientific Reports* **2021**, *11*, 10356. [[CrossRef](#)]
38. Almotairy, A.R.Z.; Amer, A.M.; El-Kady, H.; Elwakil, B.H.; El-Khatib, M.; Eldrieny, A.M. Nanostructured  $\gamma$ -Al<sub>2</sub>O<sub>3</sub> Synthesis Using an Arc Discharge Method and its Application as an Antibacterial Agent against XDR Bacteria. *Inorganics* **2023**, *11*, 42. [[CrossRef](#)]
39. Bhuvaneshwari, M.; Bairoliya, S.; Parashar, A.; Chandrasekaran, N.; Mukherjee, A. Differential toxicity of Al<sub>2</sub>O<sub>3</sub> particles on Gram-positive and Gram-negative sediment bacterial isolates from freshwater. *Environ. Sci. Pollut. Res.* **2016**, *23*, 12095–12106. [[CrossRef](#)]

**Disclaimer/Publisher's Note:** The statements, opinions and data contained in all publications are solely those of the individual author(s) and contributor(s) and not of MDPI and/or the editor(s). MDPI and/or the editor(s) disclaim responsibility for any injury to people or property resulting from any ideas, methods, instructions or products referred to in the content.